# The role of each compartment in a two-compartment vertical flow reactor for ferruginous mine water treatment

**Article** *in* Water Research · June 2014

DOI: 10.1016/j.watres.2014.05.016 · Source: PubMed

WATER RESEARCH 62 (2014) 11–19

Available online at www.sciencedirect.com

ScienceDirect

journal homepage: www.elsevier.com/locate/watres

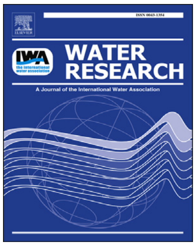

# The role of each compartment in a two-compartment vertical flow reactor for ferruginous mine water treatment

G.J. Yim [a], Y.W. Cheong [a], J.H. Hong [b], W. Hur [c,*]

[a] Geologic Environment Division, Korea Institute of Geoscience and Mineral Resources, 92 Gwahang-no, Yuseong-gu, Daejeon 305-350, Republic of Korea
[b] Mine Reclamation Corporation, 389-14 Seonghwan-eup Cheonan-si, Chungcheongnam-do 331-803, Republic of Korea
[c] Dept. of Bioengineering and Technology, Kangwon National University, 192-1 Hyoja-dong, Chuncheon, Kangwon-do 200-701, Republic of Korea

ARTICLE INFO

*Article history:*
Received 7 October 2013
Received in revised form
24 April 2014
Accepted 12 May 2014
Available online 2 June 2014

*Keywords:*
Vertical flow reactor
Mathematical model
Ochre filtration
Ferruginous mine water

## ABSTRACT

A vertical flow reactor (VFR) has been suggested for remediation of ferruginous mine drainage that passes down through an accreting bed of ochre. However, a VFR has a limited operation time until the system begins to overflow. In this study, a mathematical model was developed as a part of the effort to explore the operation of a VFR, showing dynamic changes in the head differences, ochre depths, and Fe(II)/Fe(III) concentrations in the effluent flow. The analysis showed that VFR operation time extended from 148.5 days to 163 days in an equally divided and to 168.4 days in asymmetrically (0.72:0.28) divided two-compartment VFR, suggesting that an optimum compartment ratio exists that maximizes the VFR operation time. A constant head filtration in the first compartment maximized filtration efficiency and thus prolonged VFR longevity in the two-compartment VFR. Fe(II) oxidation and ochre formation should be balanced with the permeability of the ochre bed to maximize the VFR operation time and minimize the residual Fe(II) in the effluent. Accelerated Fe(II) oxidation affected the optimum ratio of the compartment area and reduced the residual Fe(II) in the effluent. The VFR operation time can be prolonged significantly from 764 days to 3620 days by increasing the rate of ochre formation, much more than by accelerating the Fe(II) oxidation. During the prolonged VFR operation, ochre formed largely in the first compartment, while overflowing mine water with reduced iron content was effectively filtered in the second compartment. These results not only provide a better understanding of VFR operation but also suggest the direction of evolution of two-compartment VFR toward a compact and highly efficient facility integrated with an aerated cascade and with automatic coagulant feeding.

---

* *Corresponding author*. Department of Bioengineering and Technology, Kangwon National University, 192-1 Hyoja-dong, Chuncheon 200-701, Republic of Korea. Tel.: +82 33 250 6276; fax: +82 33 243 6350.
E-mail address: wonhur@kangwon.ac.kr (W. Hur).
http://dx.doi.org/10.1016/j.watres.2014.05.016
0043-1354/

### Nomenclature

| | |
|---|---|
| $A_i$ | floor area of $VFR_i$ ($m^2$) |
| $C_{Fe}$ | Fe(II) concentration of AMD influent (mg $L^{-1}$) |
| $C_{iF2}$ | Fe(II) concentration in $VFR_i$ (mg $L^{-1}$) |
| $C_{iF3}$ | Fe(III) concentration in $VFR_i$ (mg $L^{-1}$) |
| $H_i$ | hydraulic head of mine water in $VFR_i$ (m) |
| $K_i$ | overall hydraulic conductivity of the filter bed of $VFR_i$ ($day^{-1}$) |
| $K_{och}$ | hydraulic conductivity of the ochre bed (m $day^{-1}$) |
| $K_{sand}$ | hydraulic conductivity of the sand bed (m $day^{-1}$) |
| $k_1$ | pseudo first-order rate constant for Fe(II) iron oxidation ($day^{-1}$) |
| $k_2$ | pseudo first-order rate constant for ochre formation ($day^{-1}$) |
| Q | mine water flow rate ($m^3$ $day^{-1}$) |
| $q_i$ | flow rate passing down through the ochre bed in $VFR_i$ ($m^3$ $day^{-1}$) |
| $s_B$ | sand bed depth (m) |
| $VFR_i$ | vertical flow reactor *i* |
| $w$ | overflow from $VFR_1$ to $VFR_2$ ($m^3$ $day^{-1}$) |
| $x_{Bi}$ | ochre depth in $VFR_i$ (m) |
| $\rho$ | apparent density of the ochre bed (kg $m^{-3}$) |

*Subscripts*

| | |
|---|---|
| *i* | compartment number |
| iF2 | Fe(II) ion in compartment *i* |
| iF3 | Fe(III) ion in compartment *i* |

## 1. Introduction

Acid mine drainage is a persistent environmental problem. Thus, various passive treatment techniques have been developed to remediate acidic mine drainage from closed mines (Mitsch and Wise, 1998; Gazea et al., 1996). Lagoons and oxidation ponds are widely used passive treatment methods, designed so that the mine water resides in an open containment area, allowing oxidation and precipitation (Johnson and Hallberg, 2005). Oxidation of Fe(II) occurs by surface aeration and the resulting hydrous ferric oxide forms precipitates under net alkaline or neutral conditions (Johnson, 2003). Because mine drainage has a wide range of pH and a varying spectrum of metal ions, developing appropriate design criteria for oxidation ponds to ensure cost-effective performance has been a challenge. Thus, oxidation ponds are typically designed based on an iron removal rate of 10 g $m^{-2}$ $day^{-1}$ (Hedin et al., 1994) or nominal retention time of >1 day obtained from operating data (Fennessy and Mitsch, 1989). However, the scale of a settling pond based on the nominal retention time is so large that land acquisition could be a difficult task. It is especially difficult to obtain a sufficient land area near a closed mine in steep, mountainous areas.

Sapsford and Williams (2009) demonstrated that a vertical flow reactor (VFR) passing mine drainage through an accreting bed of ochre is more efficient than conventional treatment methods. Moreover, the method of dividing a VFR into two compartments to accommodate mine drainage in one compartment while treating the overflow in the other was shown to be even more efficient than a single-compartment VFR.

In this study, a mathematical model was developed to describe the dynamic behavior of Fe(II) oxidation, ochre formation, and hydraulic head change in a two-compartment VFR. The model was used to explain why a two-compartment VFR can have a longer operation time than a single-compartment VFR or an equally divided VFR. The optimum ratio for the two compartments and the effects of the Fe(II) oxidation and ochre formation rates were also investigated to improve our understanding of VFR operation and obtain the optimum design criteria for the maximum operation time of a two-compartment VFR.

## 2. Materials and methods

### 2.1. *Configuration of two-compartment VFR*

A schematic diagram of a two-compartment VFR is shown in Fig. 1. Initially, the VFR was equally divided into two compartments with floor areas $A_1 = A_2$, each of which had a flat sand bed as the bottom floor.

Surface aeration is assumed to be responsible for oxidation of Fe(II) to Fe(III) in mine water. Fe(III) is quickly converted to hydrous ferric oxide in near-neutral mine water and settles down to the ochre layer at the top of the sand bed. As mine water passes down through the sand bed, ochre accretion occurs and permeability decreases. The ochre bed was assumed to have a freely diffusible porous structure. The ochre permeability and hydraulic head determined the flow rate of mine water passing down through the ochre bed, as described by Darcy's Law:

$$q = KA\frac{\Delta H}{x_B} \tag{1}$$

where *q* is the flow rate through ochre bed ($m^3$ $day^{-1}$), *K* is the hydraulic conductivity (m $day^{-1}$), *A* is the area of the VFR ($m^2$), $\Delta H$ designates the distance from the surface level of mine drainage to the ochre bed (*m*), and $x_B$ is the filter bed thickness (*m*). Because the underlying sand bed also provides hydraulic resistance to the flow passing down, the harmonic average of the ochre and sand conductivity was used for the overall conductivity, as suggested by Reades (1989):

$$\frac{1}{K} = \frac{x_B}{K_{och}} + \frac{s_B}{K_{sand}} \tag{2}$$

where *K* is the overall conductivity ($day^{-1}$), $x_B$ is the ochre bed thickness (m), $K_{och}$ is the ochre bed conductivity (m $day^{-1}$), $s_B$ is the sand bed thickness (m), and $K_{sand}$ is the sand bed conductivity (m $day^{-1}$). In our model, $s_B$ was fixed at 0.3 m, $K_{och}$ was 0.01 m $day^{-1}$, and $K_{sand}$ was 10 m $day^{-1}$. When $x_B$ was 0.01 m, the calculated overall conductivity was $1.12 \times 10^{-5}$ $s^{-1}$, comparable to the apparent conductivity of the ochre bed estimated by Sapsford and Williams (2009). The flow (*q*)

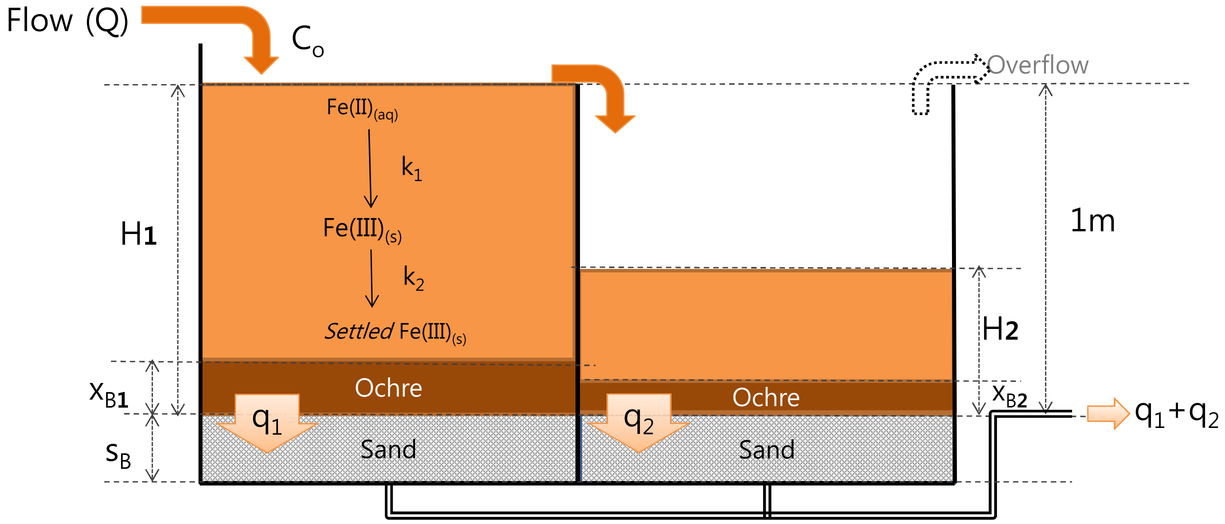

**Fig. 1 – Operational scheme of a two-compartment vertical flow reactor for ferruginous mine water treatment.**

passing down through the ochre and sand bed layers is given by

$$q = \frac{AH}{\left(\frac{x_B}{K_{och}} + \frac{s_B}{K_{sand}}\right)} \tag{3}$$

Fe(II) dissolved in mine water is oxidized to Fe(III) in the presence of dissolved oxygen. Thus, the rate law can be of the first order respect to both the concentration of Fe(II) and dissolved oxygen. However, the empirical rate law was simplified to be of the first order with respect to Fe(II) only with a pseudo first-order rate constant because of the small dependency of oxygenation rate on Fe(II) oxidation kinetics (Stumm and Lee, 1961).

Park and Dempsey (2005) reported that Fe(II) can also be oxidized heterogeneously on the surface of hydrous ferric oxide, and that the rate is faster than that of homogeneous oxidation. It is also consistent with enhanced oxidation and accretion of ochre on high surface area media in a passive treatment of ferruginous mine waters (Jarvis and Younger, 2001). Sapsford and Williams (2009) suggested a Fe(II) oxidation model composed of homogeneous Fe(II) oxidation in mine water above the ochre bed as a continuous reactor and heterogeneous Fe(II) oxidation in the ochre bed as a plug-flow reactor. However, heterogeneous Fe(II) oxidation was not considered in the present model, because parameters such as ochre density and permeability were not determined empirically for a specific VFR. In the present mathematical model, ochre formation from Fe(II) is lumped into two reactions with pseudo first-order reaction kinetics. The rate constants of Fe(II) oxidation and ochre formation were 3.72 and 12.5 day$^{-1}$, as suggested by Sapsford and Watson (2011).

Fe(III) is converted to hydrous ferric oxide, $Fe_2O_3 \cdot xH_2O$, where $x$ may vary. Hydrous ferric oxide forms flocs that gradually settle to the ochre bed. The precipitation of hydrous ferric oxide is too complex to identify each mechanism and/or the rate law of the series of reactions. Thus, the iron ion oxidation equation in mine water is often simplified to Fe(II) oxidation and ochre formation (Sapsford and Watson, 2011). In this study, we used a two-stage reaction formula:

$$\mathrm{Fe(II)_{aq}} \xrightarrow{k_1} \mathrm{Fe(III)_s} \xrightarrow{k_2} \mathrm{SettledFe(OH)_3} \tag{4}$$

where $k_1$ is the pseudo first-order rate constant of $\mathrm{Fe(II)_{aq}}$ oxidation (day$^{-1}$) and $k_2$ is the pseudo first-order rate constant of ochre formation from Fe(III) (day$^{-1}$).

### 2.2. *Mathematical model*

The hydraulic head ($H_1$) change in $VFR_1$ can be expressed as the difference between the rate of mine water input and rate of flow passing through the ochre bed filter, given by

$$\frac{dH_1}{dt} = \frac{Q}{A_1} - \frac{H_1}{x_{B1}/K_{och} + s_B/K_{sand}} \tag{5}$$

where $H_1$ is the hydraulic head of the mine water in $VFR_1$ ($m$), Q is the inlet mine water flow rate (m$^3$ day$^{-1}$), $A_1$ is the floor area of $VFR_1$ (m$^2$), and $x_{B1}$ is the ochre bed thickness in $VFR_1$ ($m$). Fe(II) concentration is not homogeneous in the compartment because of surface aeration and the geometric configuration of inlet ports. However, the Fe(II) concentration was assumed to be homogenous in our VFR to simplify the mathematical model. The mass balance of the Fe(II) concentration is determined by the rate of Fe(II) supply from the inlet flow, the rate of Fe(II) oxidation, and Fe(II) dilution rate, as follows:

$$\frac{dC_{1F2}}{dt} = \frac{QC_{Fe}}{H_1A_1} - k_1C_{1F2} - \frac{QC_{1F2}}{H_1A_1} \tag{6}$$

where $C_{1F2}$ is the Fe(II) concentration in $VFR_1$ (mg L$^{-1}$) and $C_{Fe}$ is the Fe(II) concentration in the inlet mine water (mg L$^{-1}$).

In the same way, the rate of Fe(III) concentration in $VFR_1$ is determined by the following mass balance:

$$\frac{dC_{1F3}}{dt} = k_1C_{1F2} - k_2C_{1F3} - \frac{QC_{1F3}}{H_1A_1} \tag{7}$$

where $C_{1F3}$ is the Fe(III) concentration in $VFR_1$ (mg $L^{-1}$) and $k_2$ is the pseudo first-order rate constant of ochre formation. The rate of ochre formation in $VFR_1$ is proportional to the Fe(III) concentration. Although hydrous ferric oxide ($Fe_2O_3 \cdot xH_2O$) may have a varying number of water molecules, it was assumed to be $Fe_2O_3 \cdot H_2O$ in our model. Thus, the stoichiometric conversion factor of 1.91 was obtained by dividing the molecular weight of $Fe(OH)_3$ by that of Fe(III). Accordingly, rate of increase of ochre thickness is given by

$$\frac{dx_{B1}}{dt} = 1.91\frac{H_1 k_2 C_{1F3}}{\rho} \tag{8}$$

where $x_{B1}$ is the ochre depth in $VFR_1$ ($m$) and $\rho$ is the ochre density (kg $m^{-3}$), assumed to be 500 kg $m^{-3}$ from the apparent density of ochre samples ranging between 0.35 kg $L^{-1}$ and 0.6 kg $L^{-1}$.

When mine water in $VFR_1$ overflows to the second compartment ($VFR_2$), a constant hydraulic height is maintained in $VFR_1$ while that in $VFR_2$ increases with time. The overflow rate ($w$) from $VFR_1$ to $VFR_2$ can be obtained from the difference between the inlet flow rate and the flow rate passing down through the ochre bed, as follows:

$$\text{If } H_1 > 1, \quad w = Q - \frac{A_1 H_1}{{}^{x_{B1}}/_{k\_och} + {}^{s_B}/_{K_{sand}}} \tag{9}$$

As in $VFR_1$, the hydraulic head, Fe(II) and Fe(III) concentrations, and ochre depth in $VFR_2$ can be calculated with the mass balance equations shown below. The rate of the hydraulic head change in $VFR_2$ is given by

$$\frac{dH_2}{dt} = \frac{w}{A_2} - \frac{H_2}{{}^{x_{B2}}/_{K_{och}} + {}^{s_B}/_{K_{sand}}} \tag{10}$$

where $H_2$ is the hydraulic head of the mine water in $VFR_2$ (m), $w$ is the overflow rate ($m^3$ $day^{-1}$), $A_2$ is the floor area of $VFR_2$ ($m^2$), and $x_{B2}$ is the ochre bed thickness in $VFR_2$ (m). The rate of Fe(II) oxidation in $VFR_2$ is given by

$$\frac{dC_{2F2}}{dt} = \frac{wc_{1F2}}{H_2 A_2} - k_1 C_{2F2} - \frac{wC_{2F2}}{H_2 A_2} \tag{11}$$

where $C_{2F2}$ is the Fe(II) concentration in $VFR_2$ (mg $L^{-1}$). The rate of Fe(III) oxidation in $VFR_2$ is given by

$$\frac{dC_{2F3}}{dt} = k_1 C_{2F2} - k_2 C_{2F3} - \frac{wC_{2F3}}{H_2 A_2} \tag{12}$$

where $C_{2F3}$ is the Fe(III) concentration in $VFR_2$ (mg $L^{-1}$). The depth of the ochre in $VFR_2$ is determined by the Fe(III) concentration, as given by

$$\frac{dx_{B2}}{dt} = 1.91\frac{H_2 k_2 C_{2F3}}{\rho} \tag{13}$$

where $x_{B2}$ is the ochre depth in $VFR_2$ ($m$).

The series of differential equations given by (5)–(13) were used as a mathematical model for a two-compartment VFR. After overflow occurred in $VFR_1$, equation (5) was replaced by $dH_1/dt = 0$. The initial values of $H_1$ and $H_2$ were assigned to be 0.001 m, while those of $x_{B1}$ and $x_{B2}$ were assigned to be 0.001 m. A numerical solution of the ordinary differential equations was obtained using Matlab (Mathworks, Natick, MA, USA).

## 3. Results

### 3.1. *Dynamic changes in a two-compartment VFR*

The mathematical model developed in the previous section was used to calculate the mine water levels, Fe(II) concentrations, and ochre depth in each compartment of a two-compartment VFR using the parameters listed in Table 1, when inlet flow rate of mine water was 1.5 $m^3$ $day^{-1}$ and the Fe(II) concentration was 10 mg $L^{-1}$ (Fig. 2). The mine water level in $VFR_1$ rose rapidly, 0.3 m in a half-day, and then increased gradually to 1 m at 68.9 days. After overflow occurred from $VFR_1$ to $VFR_2$, the water level in $VFR_2$ increased gradually to 1 m after 289.7 days of operation. The flow through the ochre bed had a maximum rate of 1.497 $m^3$ $day^{-1}$ at 1.1 days, which was reduced to 1.492 $m^3$ $day^{-1}$ at 68.9 days of operation, indicating that the inlet mine water (1.5 $m^3$ $day^{-1}$) mostly passed down through the ochre bed in $VFR_1$ before overflow occurred. After overflow occurred, the cumulative flow through the first ochre bed corresponded to 43.4% of the total flow filtered through both ochre beds.

The Fe(II) in $VFR_1$ decreased from 10 to 7.2 mg $L^{-1}$ during the first half-day of operation, coinciding with the period of initial development of the ochre bed. The Fe(II) concentration decreased gradually to 4.5 mg $L^{-1}$ when overflow occurred in $VFR_1$, and remained constant after that time. Upon mine water overflowing into $VFR_2$, both the Fe(II) and ferric oxide levels increased sharply and then started to decline. Since the effluent flow consisted of the merged flows filtered through both ochre beds, the effluent ferric oxide and Fe(II) concentrations over time are shown in Fig. 2f. Fe(II) was not effectively removed during the early part of the VFR operation because the ochre accretion was not enough to provide sufficient residence time. The ferric oxide concentration in the effluent flow was approximately 1 mg $L^{-1}$ throughout the operation period of the VFR.

The hydraulic performance of the two-compartment VFR demonstrated by the mathematical model helps in understanding the operational properties in each sector. Although the VFR was divided equally, overflow occurred far earlier than half of the total operation span. After that, constant head filtration was achieved in the first compartment which maximizes filtration efficiency resulting in a much higher ochre depth than the second. However, the presence of Fe(II) in the second compartment indicated that the Fe(II) oxidation may be a rate-limiting step in the two compartment VFR model with the kinetic parameters of Table 1.

**Table 1 – Parameters used for the calculations.**

| Parameter | Value | |
|---|---|---|
| $C_{Fe}$ | 10–50 mg $L^{-1}$ | (Sapsford and Watson, 2011) |
| $k_1$ | 3.75 $day^{-1}$ | (Sapsford and Watson, 2011) |
| $k_2$ | 12.5 $day^{-1}$ | |
| $K_{och}$ | 0.01 m $day^{-1}$ | |
| $K_{sand}$ | 10 m $day^{-1}$ | |
| $P$ | 500 kg $m^{-3}$ | |
| $s_B$ | 0.3 m | |

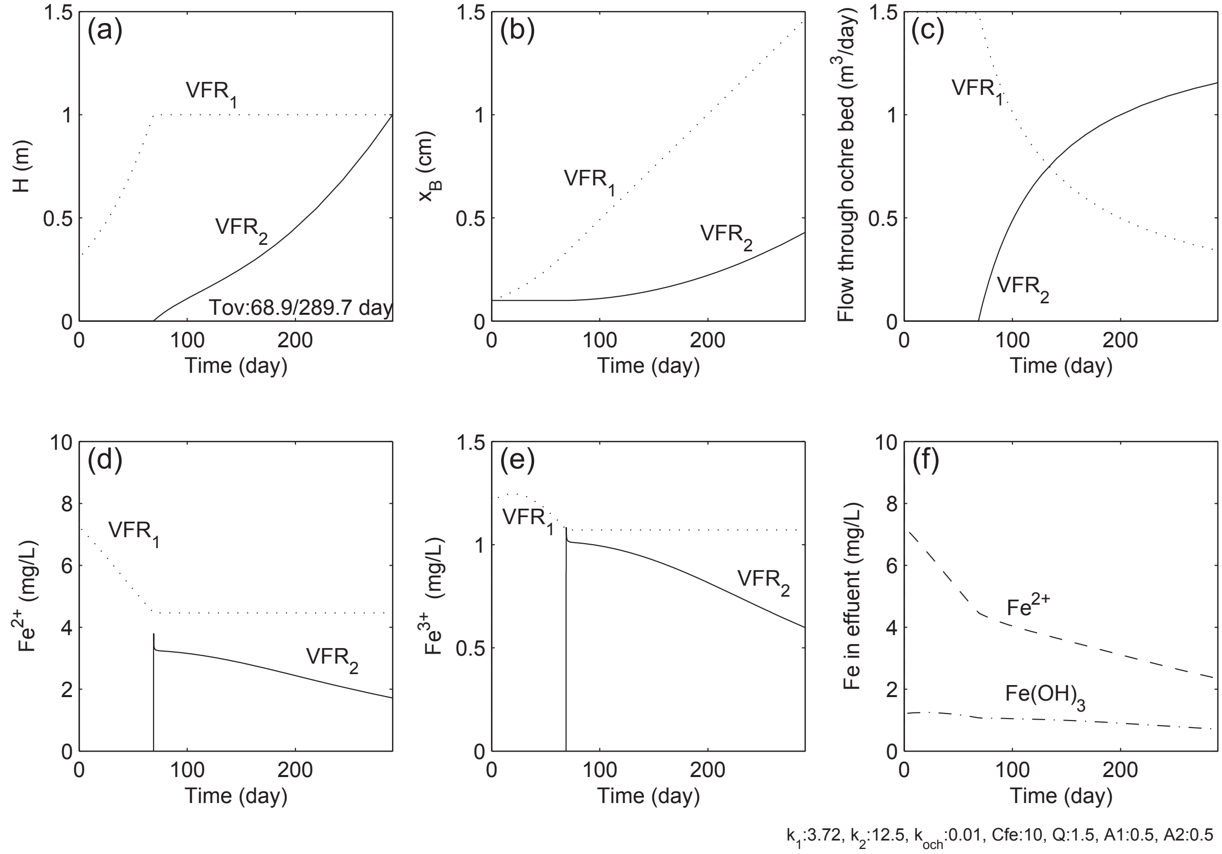

**Fig. 2 – (a–e) Dynamic changes in hydraulic heads with VFR operation time (Tov), ochre depth, filtrates, and Fe(II) and Fe(III) concentrations in each VFR. (f) Fe(II) and hydrous ferric oxide concentrations in VFR2 effluent.**

### 3.2. *Fe(II) oxidation, ochre accretion, and filtration balance*

Because our calculations predicted a significant level of residual Fe(II), Fe(II) oxidation appears to be a rate-limiting at the pseudo first-order rate constant of 3.75 $\text{day}^{-1}$. With these increments in the oxidation rate to 10, 100, and 1000 $\text{day}^{-1}$, the VFR overflow time decreased slightly from 289.7 to 240.6, 261.2, and 274.2 days, respectively (Fig. 3). However, the Fe(II) levels in the effluent decreased significantly from 2.34 to 0.81, 0.05, and 0.00 $\text{mg L}^{-1}$, respectively, at the time of overflow. The ochre depths increased from 1.5 to 1.7, 1.9, and 2.1 cm, respectively, in $VFR_1$, while those in $VFR_2$ did not change significantly.

These results indicate that an increased oxidation rate forms a thicker ochre bed in $VFR_1$, which contributes to purification of the water in two ways. As more Fe(II) is converted to ochre and the ochre layer becomes thicker, the suspended solids in mine water are expected to be clarified more efficiently when passing through the thickened ochre bed. The overflow times in $VFR_1$ were also shortened to 66.1, 47.4, 38.1, and 33.4 days, corresponding to 23, 19, 16, and 14%, respectively, of the total operation span. The overflow in $VFR_1$ occurred earlier as the oxidation rate increased. After overflow occurred, the first compartment continued to contribute to purification of the mine water by constant-head filtration during the rest of the operation span. The percentages of effluent passing down through the first compartment were 56.5, 51.8, 47.2, and 43.3%, depending on the rate constants of Fe(II) oxidation.

### 3.3. *Optimum compartment ratio to maximize VFR operation*

The previous results indicate that ochre accretion occurred mostly in $VFR_1$ and that constant-head filtration occurred over a large portion of the $VFR_1$ operation. The water level in $VFR_2$ rose slowly because of the low level of residual Fe(II) and the thin ochre depth in $VFR_2$. Both compartments participated in mine water purification, but by different modes. Thus, it is expected that the compartment ratio will influence the VFR operation. The mathematical model was used to calculate the VFR overflow time for varying compartment area ratios. The calculated overflow time had maximum and minimum values when the area ratios of the first compartment ($A_1/A$) were 0.716 and 0.109, respectively (Fig. 4a). The VFR operation time had its maximum value of 168.4 days, higher than the 145.8 days calculated for a single-compartment VFR, when $A_1/A$ was 0 or 1.

The profile of VFR operation time was also calculated with various flow rates, iron contents, and ochre permeability. When the inlet flow rate was reduced from 2 to 1 $\text{m}^3\ \text{m}^{-2}\ \text{day}^{-1}$, this resulted in a prolonged VFR operation time of 668.9 days at a compartment ratio of 0.605 (Fig. 4b). Fig. 4c shows that the VFR operation time decreased with increasing iron

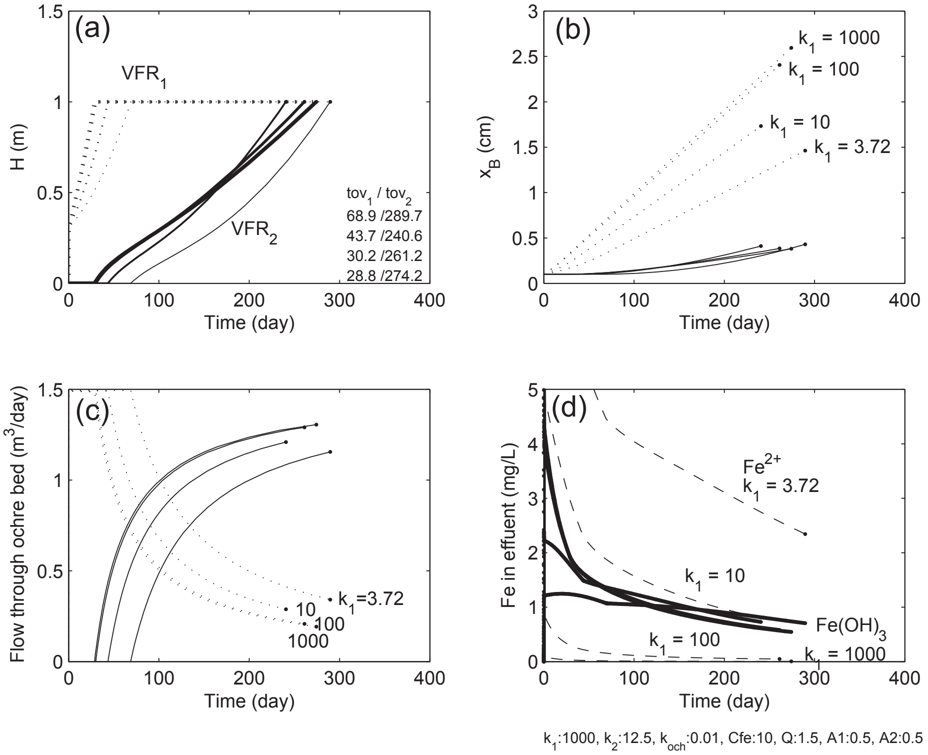

**Fig. 3** – **Dynamics of the (a) hydraulic head, (b) ochre depth, (c) mine water flow rates passing down through the ochre bed, and (d) Fe(II) and ferric oxide concentrations in the effluent.**

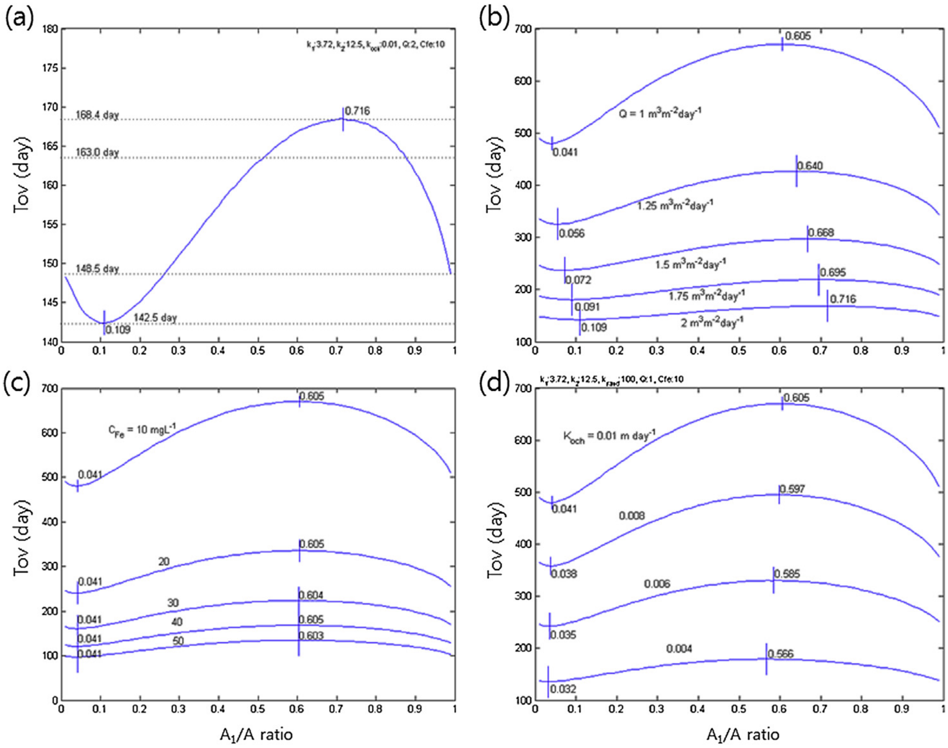

**Fig. 4** – **VFR operation time (Tov) with (a) varying compartment ratios, at different (b) flow rates, (c) Fe(II) concentrations, and (d) ochre hydraulic conductivities.**

content in the inlet mine water, but the optimum ratio that maximized the VFR operation time ranged from 0.605 to 0.603. Decreasing the ochre permeability also reduced the VFR operation time (Fig. 4d).

These results demonstrate that the VFR operation time can be prolonged by adjusting the area ratio of the first and second compartments. The area ratio that maximized the VFR operation period ranged from 0.716 to 0.556, depending on the other parameters, such as inlet flow rate, Fe(II) content, and ochre permeability.

### 3.4. *Accelerated Fe(II) oxidation*

It was shown that the VFR operation time varied depending on the area ratio of the two compartments. Therefore, the VFR operation time was calculated for varying area ratios under accelerated Fe(II) oxidation conditions. The pseudo first-order rate constant ($k_1$) of the Fe(II) oxidation reaction was increased from 3.75 to 10, 100, 1000 and 10,000 $\text{day}^{-1}$, while the rate constant ($k_2$) of the ochre formation bed was fixed at 12.5 $\text{day}^{-1}$. Fig. 5 shows that the area ratio that maximized the VFR operation time changed from 0.667 to 0.559, 0.433, 0.413, and 0.411, respectively, while the maximum VFR operation time decreased from 296.3 to 241.7, 263.7, 279.1, and 280.9 days, respectively.

Accelerated Fe(II) oxidation reduced the maximum VFR operation time due to the increased ochre formation in $VFR_1$. The increased ochre formation was not only attributed to the reduced VFR operation time, but also to the lower residual Fe(II) concentration in the effluent, as shown above for an equally divided VFR (Fig. 3). The optimum area ratio maximizing the VFR operation time changed from 0.667 to 0.411 with increasing Fe(II) oxidation rate. This analysis shows that the rate of Fe(II) oxidation significantly affected the optimum area ratio that maximized the operation time in a two-compartment VFR.

### 3.5. *Rate of ochre formation*

The previous results show that accelerated Fe(II) oxidation reduced the residual Fe(II) in the effluent, but it did not increase the VFR operation time. This suggests that the subsequent reaction that form the ochre bed may be rate limiting. Thus, the VFR operation time was also calculated when $k_1$ was assumed to be 100 $\text{day}^{-1}$ while $k_2$ was raised from 12.5 to 100, 1000, and 10,000 $\text{day}^{-1}$. Fig. 6 shows that the VFR operation time increased significantly from 263.7 to 579.5, 956.6, and 1035.2 days, respectively, and the optimum compartment ratio varied from 0.433 to 0.347, 0.328, and 0.326, respectively. Thus, the operation time could be prolonged by up to 3.7 times with an increased ochre formation rate.

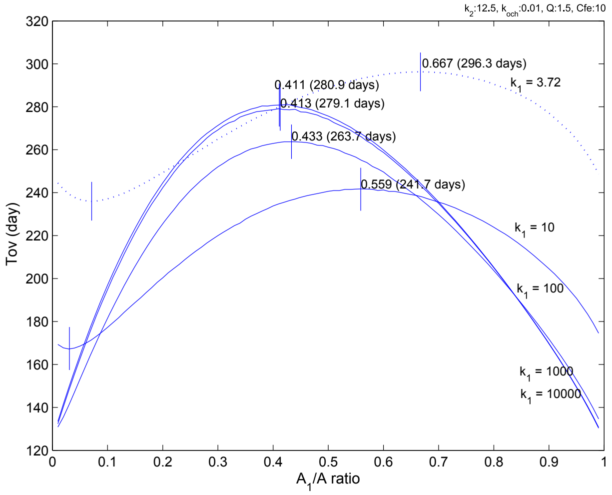

**Fig. 5 – VFR operation time (Tov) for varying $A_1$/A ratios with different pseudo first-order kinetic parameters for Fe(II) oxidation.**

These results show that rapid ochre formation is critical for extended operation of a VFR. Fig. 7 illustrated how the VFR operation time is significantly prolonged, showing the modeled dynamic behavior of a two-compartment VFR with $k_1 = 100\ \text{day}^{-1}$ and $k_2 = 10{,}000\ \text{day}^{-1}$. Rapid ochre formation resulted in early overflow in $VFR_1$ at 7.2 days and a low level of Fe(II) in $VFR_2$. Thus, the mine water passed down through a thin ochre bed in $VFR_2$ for a long period of time. At the end of the VFR operation, the ochre depth of $VFR_1$ was 17.5 cm while that of $VFR_2$ was 0.44 cm. Only 2% of the inlet mine water passed down through $VFR_1$, while 98% of the mine water overflowed to $VFR_2$ and passed down through the ochre bed in $VFR_2$.

It is not feasible to raise the ochre formation rate constant up to 10,000 $\text{day}^{-1}$, but a mathematical simulation under extreme conditions can readily explain how VFR operation can be extended: ochre forms largely in the first compartment, while overflowing mine water with a reduced iron content is effectively filtered in the second compartment. The VFR operation time was more significantly prolonged as the ochre formation increased compared to any other parameter in the present model. Thus, methods to facilitate ochre formation are worthy of further exploration.

## 4. Discussion

A VFR is an interesting continuous system where an oxidation product serves as a filtration material. Thus, effective purification of ferruginous mine water can be achieved when the

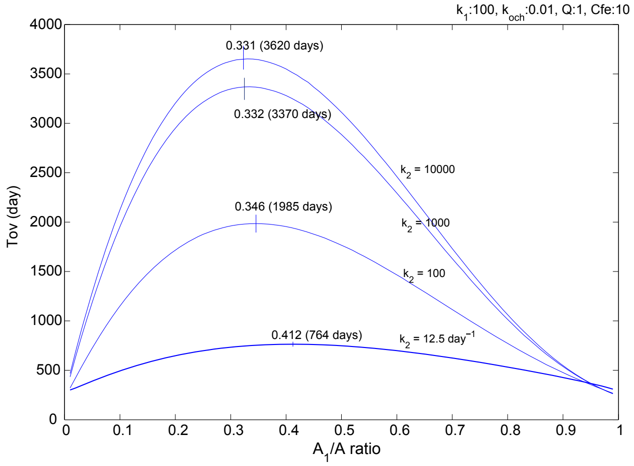

**Fig. 6 – VFR operation time for varying $A_1$/A ratios with different pseudo first-order rate constants of ochre formation.**

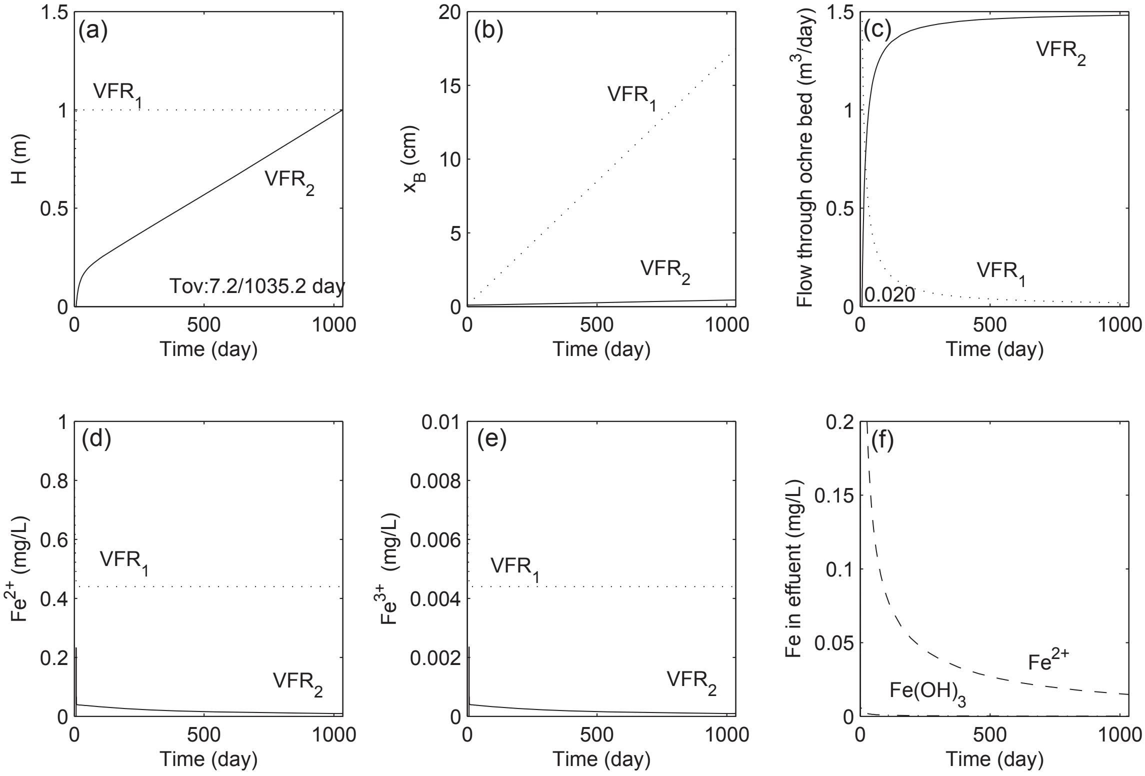

$k_1$:100, $k_2$:10000, $k_{och}$:0.01, Cfe:10, Q:1.5, A1:0.326, A2:0.674

**Fig. 7 – (a–e) Dynamic changes in hydraulic heads, ochre depth, filtrates, and Fe(II) and Fe(III) concentrations in each VFR. (f) Fe(II) and hydrous ferric oxide concentrations in $VFR_2$ effluent.**

oxidation rate keeps pace with the hydraulic performance. The rate of Fe(II) oxidation in mine water has been modeled by using the equation (14) and the overall rate constant ($k_1$) was estimated to be 1.5 × $10^{13}$ $M^{-2}$ $atm^{-1}$ $min^{-1}$ (Stumm and Lee, 1961).

$$\frac{d[Fe(II)]}{dt} = k_1[Fe(II)]P_{O_2}[OH^-]^2 \tag{14}$$

The Fe(II) oxidation rate constant can be converted to 0.43 $day^{-1}$ at pH 6 and to 43.2 $day^{-1}$ at pH 7 in the form of pseudo-first order rate constant with respect to Fe(II) concentration under ambient pressure. The pseudo-first order rate constant (3.72 $day^{-1}$) used in the present simulation lies in between the two values. However, Geroni and Sapsford (2011) reported that the rate constants in the field are 1–3 orders of magnitude higher than those reported by laboratory studies, because of heterogeneous oxidation of Fe(II). The suggested values in the range of 2.7 × $10^{14}$–2.7 × $10^{16}$ $M^{-2}$ $atm^{-1}$ $min^{-1}$ correspond to the pseudo-first order rate constants in the range of 7.78–778 $day^{-1}$ at pH 6. It suggests that Fe(II) oxidation rate can increase by several orders of magnitude depending on the pH and on the contribution of heterogeneous oxidation. Thus, the effect of accelerated Fe(II) oxidation by the orders of magnitude was demonstrated in Figs. 3 and 5. The resulting hydrous ferric oxide flocculates and settles down to form an ochre bed to clarify mine water. Settling rate is different for different mine water and known to be 12.5 $day^{-1}$ as an upper limit of pseudo first-order rate constant with respect to Fe(III) concentration (Sapsford, 2013). Ochre accretion deteriorates the hydraulic performance of the filter bed. Therefore, VFR has a limited life span until it reaches overflow. Estimation of longevity using the mathematical model presented in this report, is important in VFR design because an optimum design that maximizes VFR operation could save on initial capital investment. The present approach can suggest a proper time for ochre removal in a full-scale VFR operation.

The present analysis explains why a two-compartment system has a longer operation time, and shows the presence of an optimum ratio to divide VFR into two compartments. Rapid ochre accretion in the first compartment maintained a constant hydraulic head to maximize the flow passing down through the ochre bed. The filtration rate in the second compartment was also facilitated by a thin ochre bed because of lower residual Fe(II) in the overflow. Balancing of Fe(II) oxidation, ochre formation and filtration processes is more complicated in a two-compartment VFR, suggesting the presence of an optimum compartment ratio. The optimum ratio is very dependent to the kinetic parameters in Fe(II) oxidation and ochre formation. The simulation presented that VFR longevity significantly increased from 290 day (Fig. 3) to 3620 days (Fig. 6) under accelerated Fe(II) oxidation and rapid ochre formation conditions. Since Fe(II) oxidation rate in the field appeared higher, the present analysis guides the direction of VFR evolution to a high through-put treatment facility with an automated coagulant feeding for rapid ochre precipitation.

Two-compartment VFR operation is simulated using a proposed mathematical model with simplified kinetics and fixed hydraulic conductivity. Thus, apparent rate of Fe(II) oxidation and ochre formation could be different from the proposed rate laws in the present model in the presence of significant concentration gradient of reaction components. In addition to that, ochre compression should also be taken into consideration for more accurate prediction of the growth of cakes and filtration, as suggested by Stamatakis and Tien (1991). Heterotrophic iron-oxidizing filamentous bacteria have been found in the iron ochre of drainage systems (Wheatley, 1988); this is also expected to influence the ochre permeability. The ochre density and ferric oxide must be determined empirically to allow application of the proposed mathematical model to a specific VFR. Singh et al. (1999) reported that ferrihydrite ($Fe_2O_3 \cdot 0.5H_2O$) and goethite (αFeOOH) are the major components in ochre sediment from acid mine drainage in the UK. Other ochre is reportedly composed of goethite and lepidocrocite (βFeOOH).

The present study suggested that the VFR operation time can be significantly prolonged by increasing the rate of ochre formation when Fe(II) oxidation is not rate limiting. Thus, a VFR design should aim to increase the residence time, and facilitate ochre formation and Fe(II) oxidation. A VFR is an effective passive treatment system compared with a conventional oxidation pond, but there is room for further development to create a more efficient longer-lasting system.

## 5. Conclusions

A mathematical model was developed to simulate VFR operation, showing dynamic changes in head differences, ochre depth, and Fe(II)/Fe(III) concentrations in the effluent flow. Analysis of two-compartment VFR model indicated that rapid ochre accretion in the first compartment maintained a constant hydraulic head to maximize the flow passing down through the ochre bed and thus facilitate high filtration rate because of lower residual Fe(II) in the second compartment. It also shows that the compartment ratio also significantly affected the operation span of a two-compartment VFR. Accelerated Fe(II) oxidation significantly affected the optimum ratio of the compartment area and reduced the residual Fe(II) in the effluent. The analysis suggests that VFR operation time could be prolonged significantly by increasing the rate of ochre formation since Fe(II) oxidation rate can be 1–3 orders of magnitude higher in the field.

## Acknowledgements

This research was supported by MIRECO, by the Basic Research Project (14-3212) of KIGAM, and by 2014 research grant from Kangwon National University (C1010753-01-01).

## REFERENCES

Fennessy, M.S., Mitsch, W.J., 1989. Treating coal mine drainage with an artificial wetland. Res. J. Water Pollut. Control Fed. 61, 1691–1701.

Gazea, B., Adam, K., Kontopoulos, A., 1996. A review of passive systems for the treatment of acid mine drainage. Min. Eng. 9 (1), 23–42.

Geroni, J.N., Sapsford, D.J., 2011. Kinetics of iron (II) oxidation determined in the field. Appl. Geochem 26, 1452–1457.

Hedin, R.S., Nairn, R.W., Kleinmann, R.L.P., 1994. Passive Treatment of Coal Mine Drainage. US Bureau of Mines IC9389, Pittsburgh, PA, USA, p. 35.

Jarvis, A.P., Younger, P.L., 2001. Passive treatment of ferruginous mine waters using high surface area media. Water Res. 35 (15), 3643–3648.

Johnson, D.B., 2003. Chemical and microbiological characteristics of mineral spoils and drainage waters at abandoned coal and metal mines. Water Air Soil. Pol. Focus 3 (1), 47–66.

Johnson, D.B., Hallberg, K.B., 2005. Acid mine drainage remediation options: a review. Sci. Total Environ. 338 (1), 3–14.

Mitsch, W.J., Wise, K.M., 1998. Water quality, fate of metals, and predictive model validation of a constructed wetland treating acid mine drainage. Water Res. 32 (6), 1888–1900.

Park, B., Dempsey, B.A., 2005. Heterogeneous oxidation of Fe (II) on ferric oxide at neutral pH and a low partial pressure of $O_2$. Environ. Sci. Technol. 39 (17), 6494–6500.

Reades, D.W., 1989. The Results of On-going Monitoring of the Performance of a Low Permiability Clay Liner, Keele Valley Landfill, Maple, Ontario. Geotechnical Research Centre, University of Western Ontario, London.

Sapsford, D.J., Williams, K.P., 2009. Sizing criteria for a low footprint passive mine water treatment system. Water Res. 43 (2), 423–432.

Sapsford, D.J., Watson, I., 2011. A process-orientated design and performance assessment methodology for passive mine water treatment systems. Ecol. Eng. 37 (6), 970–975.

Sapsford, D.J., 2013. New perspectives on the passive treatment of ferruginous circumneutral mine waters in the UK. Environ. Sci. Pollut. Res. 20, 7827–7836.

Singh, B., Wilson, M.J., McHardy, W.J., Fraser, A.R., Merrington, G., 1999. Mineralogy and chemistry of ochre sediments from an acid mine drainage near a disused mine in Cornwall, UK. Clay Min. 34 (2), 301–317.

Stamatakis, K., Tien, C., 1991. Cake formation and growth in cake filtration. Chem. Eng. Sci. 46 (8), 1917–1933.

Stumm, W., Lee, G.F., 1961. Oxygenation of ferrous iron. Ind. Eng. Chem. 53 (2), 143–146.

Wheatley, R.E., 1988. Ochre deposits and associated bacteria in some field drains in Scotland. J. Soil. Sci. 39 (2), 253–264.